

# The longitudinal space charge effect and energy resolution \*

M. M. Gordon

*Michigan State University, Michigan, U.S.A.*

## 1. INTRODUCTION

In the design of isochronous cyclotrons with distinctly separated turns at extraction, calculations of energy resolution are customarily based solely on considerations of the beam phase width, the rf voltage and its resultant wave form.<sup>1</sup> Machines of this type have been proposed which aim at 100  $\mu$ A currents with an energy resolution of  $10^{-3}$  or better, and it appears quite likely that the hitherto neglected longitudinal space charge effect will determine the actual current or energy resolution achievable in such cyclotrons.<sup>2</sup> The longitudinal space charge effect was first discussed by T. A. Welton who explained how this effect tends to destroy turn separation by increasing the energy spread within a turn.<sup>3</sup> Welton also pointed out that this effect could be alleviated by accelerating the beam off the peak of the rf wave.<sup>4</sup> More recently, W. B. Powell carried out approximate calculations which indicate that the longitudinal space charge effect could nevertheless still be very serious.<sup>5</sup> The present paper summarises an extensive analysis of the longitudinal space charge effect and provides formulas for calculating the resultant energy spread within a turn under certain conditions.

The MSU cyclotron has been operating successfully in a separated turn mode with 100% extraction for the past three years and therefore constitutes a real prototype for the 'separated turn isochronous cyclotron'. Recently, the phase selection technique used in this machine has been refined so that proton beams up to 10  $\mu$ A can be obtained with a phase width of  $1.4^\circ$  (*FWHM*).<sup>6</sup> This narrow phase width implies an energy resolution of:  $\Delta E/E = 10^{-4}$  attainable under operating conditions computed to minimise this quantity at extraction.<sup>7</sup> However, the dee voltage has so far been regulated only to:  $\Delta V/V = (2 \text{ to } 6) \times 10^{-4}$ , so that this parameter restricts the energy resolution achievable in the external beam. Experimental measurements of the longitudinal space charge effect have recently been carried out for the first time in any cyclotron. Although these results are still preliminary, they demonstrate conclusively that the properly minimised energy resolution increases with beam current. The explicit calculations presented here are aimed toward accounting for these observations.

\*This work was supported by the National Science Foundation.

2. VORTEX MOTION

Consider the non-relativistic motion of a charge  $q$  in the isochronous magnetic field  $B$  as viewed in a reference frame rotating with constant angular velocity  $\underline{\omega}$  whose direction is perpendicular to  $B$  and whose magnitude is the isochronous angular frequency. If there are no electric fields present, then on a time-average basis the charge  $q$  will be at rest. Considering the electric field vector  $\underline{F}$  as a perturbation, the steady-state (non-oscillatory) velocity vector  $\underline{v}$  is then given by:

$$m_o \underline{\omega} \times \underline{v} = q\underline{F} \tag{1}$$

that is, the Coriolis force has the effect of reversing the magnetic field direction as seen by  $q$  in the rotating frame. Since this steady-state velocity is perpendicular to both  $\underline{\omega}$  and  $\underline{F}$ , it is directed along the equipotential curves associated with  $\underline{F}$ . In the rotating frame the rf electric field has a time-average component in the azimuthal direction given by:  $V_1/(2\pi r)$ , and Eqn (1) shows that this field causes the particles to move radially outward with the velocity:  $dr/dt = qV_1/2\pi m_o \omega r$ , so that  $qV_1$  is the average energy gain per turn. If the rf electric field is absent, the  $\underline{F}$  is produced entirely by the space charge and Eqn (1) indicates that the charges will then circulate clockwise about the point of maximum potential, thereby establishing a 'vortex' in the space charge cloud as viewed in the rotating frame. This vortex motion is depicted in Fig. 1. Since both electric fields are actually present, the resultant steady-state motion is a superposition of these two phenomena.

The longitudinal space charge effect has been extensively investigated for other types of accelerators.<sup>8</sup> Synchrotron oscillations as viewed in the

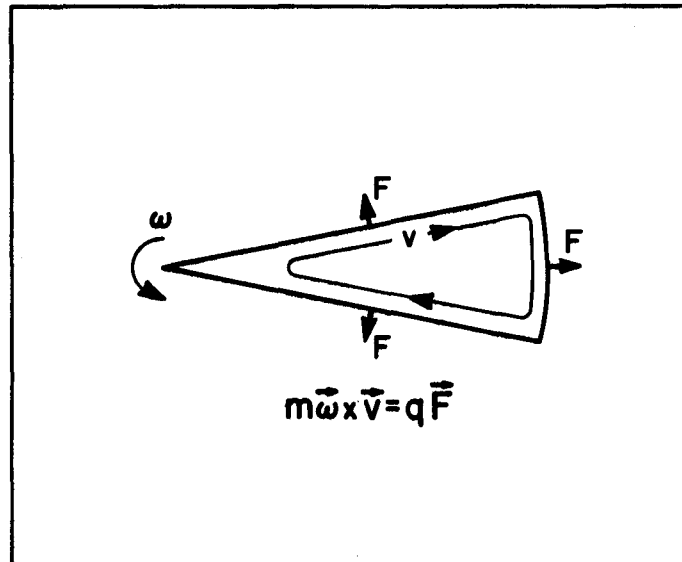


Fig. 1. Vortex motion within the space charge cloud in an isochronous cyclotron. The electric field  $F$  is that produced exclusively by the space charge itself. Angular velocity:  $\underline{\omega} = -(q/mc) \langle \underline{B} \rangle$

appropriate rotating reference frame also constitute a type of vortex motion. In a synchrocyclotron, for example, the vortex motion produced by the space charge force reinforces the vortex motion associated with the synchrotron oscillations thereby increasing the frequency of these oscillations.

### 2.1. Local vortices

In an isochronous cyclotron with separated turns the charge density and resultant electrostatic potential have local maxima at the centre of each ion bunch or turn. As a result, the central region of each turn will execute a local vortex motion in which the ions remain within the same turn; the ions outside this region, however, will partake in the overall vortex motion of the total charge cloud and it is only this motion which tends to destroy the turn separation. Since the length  $r\Delta\theta$  of the turn is generally much greater than the radius gain per turn, the local vortices are so small and feeble that their presence can be neglected entirely. This rule may not apply when the cyclotron operates under pulsed conditions; in the MSU cyclotron, for example, where nine out of ten ion pulses can be completely rejected, the radial separation between ion bunches is then always greater than the length  $r\Delta\theta$ , so that the local vortices are quite significant in this case. However, this special situation will not be treated here. It should be noted that in those cases where the vortex motion seriously changes the charge distribution, an iterated calculation may then be necessary to achieve adequate self-consistency.

## 3. ENERGY CHANGES

A properly relativistic treatment of the problem can be achieved by introducing the polar angle transformation:  $\theta = \omega t + \varphi$ , where the phase  $\varphi$  gives the azimuthal position of the particle in the rotating frame. Treating the electric fields as perturbations, the steady-state motion is then described by:

$$d\varphi/dt = - (q/m\omega R)F_r(R, \varphi), \quad (2a)$$

$$dE/dt = (qV_o\omega/2\pi) \cos \varphi + q\omega R F_\theta(R, \varphi), \quad (2b)$$

where  $m$ ,  $E$  are the relativistic mass and energy of the particle,  $R$  is the mean orbit radius,  $qV_o$  is the peak energy gain per turn produced by the rf voltage, and  $F_r$ ,  $F_\theta$  are the components of the electric field produced by the space charge. These then are the equations for the longitudinal motion appropriately modified to include the space charge force.

Assuming the field is perfectly isochronous, then the space charge cloud has the 'sector' shape depicted in Fig. 1, and  $F_r$  has an appreciable value only near  $R = 0$  and  $R = R_{\max}$ . Eqn (2a) shows that  $F_r$  acts like an error in the isochronous field given by:  $\delta B = - (c/\omega R)F_r$ , and estimates of this error for the MSU cyclotron yield:  $\delta B/B \sim 10^{-6}$  which is quite trivial. Moreover,  $F_r$  acts over relatively few turns and under these conditions only the component  $F_\theta$  will have a significant effect. If the magnetic field deviates substantially from the isochronous value as a function of radius, then there is an additional term in Eqn (2a) which produces large excursions in the values of  $\varphi$ . In such cases, the shape of the space charge cloud will be considerably deformed from the simple shape shown in Fig. 1, and the calculation of the longitudinal space charge effect:

will consequently be greatly complicated. For the 36 MeV proton field considered here later, the  $\varphi$  variation in the region of significance ( $R = 25$  to  $71$  cm) is less than  $\pm 5^\circ$ ,<sup>9</sup> and will therefore have a negligible effect. Hence, we assume hereafter that the magnetic field is perfectly isochronous and that the values of  $\varphi$  are therefore constants.

If only the space charge force is considered, then Eqn (2b) yields the following value for the energy of the particle:

$$E_{sc}(\varphi, \tau) = 2\pi q \int R F_\theta d\tau, \quad (3)$$

where:  $\tau = \omega t / 2\pi$  is the 'turn number'. Taking  $\varphi = 0$  at the azimuthal centre of the space charge distribution, it then follows from symmetry that both  $F_\theta$  and  $E_{sc}$  are odd functions of  $\varphi$  and that  $E_{sc}(\varphi = 0) = 0$ . Consequently, the space charge force causes the particles with positive/negative  $\varphi$  values to gain more/less energy than those at the central  $\varphi = 0$  value thereby increasing the energy spread within a single turn; this result coincides with that found by Welton.<sup>3</sup> The value of  $F_\theta$  falls off with increasing  $|z|$ , and if this decrease is significant, then the value of  $F_\theta$  should be properly averaged over the particle's axial oscillation before calculating  $E_{sc}$ .

The energy of the particle is:  $E = E_{sc} + E_{rf}$ , where  $E_{rf}$  is the energy acquired from the rf voltage. In the formulation of Eqn (2b) it was assumed that the particles with  $\varphi = 0$  have the maximum energy gain per turn, and this choice minimises the energy spread in the absence of the space charge force. The additional energy spread produced by the space charge force can be partially cancelled by a suitable decrease in the rf frequency. If the rf angular frequency is changed from  $\omega$  to  $\omega(1 - \epsilon)$ , then the factor  $\cos \varphi$  in Eqn (2b) is replaced by  $\cos(\varphi + \epsilon\omega t)$ , and integration of Eqn (2b) then yields:

$$E_{rf}(\varphi, \tau_0) = E_0 [\cos \varphi - (\alpha\tau_0/J) \sin \varphi], \quad (4)$$

where  $\alpha = 2\pi\epsilon$ ,  $J = 1 + (1 - \alpha^2\tau_0^2)^{1/2}$ , and  $E_0 = qV_0\tau_0$ , with  $\tau_0 = (\sin \alpha\tau)/\alpha$  being the 'original' turn number. The frequency shift method for cancelling the space charge effect has limitations. The  $\varphi$  dependence of  $E_{sc}$  and  $E_{rf}$  are generally quite different so that the cancellation can only be partial. Moreover, this frequency shift amplifies  $E_{sc}$  since it increases the total number of turns inside the cyclotron and thereby increases both the strength and duration of  $F_\theta$ . Nevertheless, the frequency shift method has been successfully used in the MSU cyclotron to maintain turn separation when the beam current is increased.

#### 4. CHARGE DENSITY

In characterising the charge density it is convenient to introduce an electric field unit:  $F_0 = IB/cDV_0$ , which is specified by the following operational parameters:  $I$  = time-average beam current,  $B = (m_0c\omega/q)$ ,  $D = \text{duty-factor} = \Delta\theta/2\pi$ , and  $V_0$  is given in Eqn (2b). In terms of conventional units, we have:

$$F_0 (V/m) = (0.9)I(\mu A)B(kG)/DV_0(kV), \quad (5)$$

where the symbols in parentheses give the units for each quantity. For the 36 MeV proton beam considered later with:  $I = 7.2 \mu A$ ,  $\Delta\theta = 1.4^\circ$ ,  $B = 11.4$  kG, and  $V_0 = 170$  kV, we have:  $F_0 = 110$  V/m.

Ignoring temporarily the discrete turn structure in the sector-shaped space charge cloud (Fig. 1), the charge density  $\rho$  can be written as:

$$\rho(R, \varphi, z) = F_0(\Delta\theta) K(R) \sigma_2(\varphi) \sigma_3(z), \quad (6)$$

assuming that the functional dependence of  $\rho$  can be split into three separate factors and where:  $\int \sigma_2(\varphi) d\varphi = \int \sigma_3(z) dz = 1$ ,  $K(R) = (V_0/V_1)\gamma^3$ , with  $\gamma = (1 - \omega^2 R^2/c^2)^{-1/2}$  and  $qV_1$  is the actual energy gain per turn. If the angular width of the beam is sufficiently large to make the  $\varphi$  dependence of  $V_1$  significant, then this dependence should be incorporated into  $\sigma_2(\varphi)$ . For conditions obtaining in the MSU cyclotron, the  $\varphi$  dependence of  $V_1$  is insignificant. The phase distribution within the internal beam has been measured and found to be symmetric and triangular in shape with  $\Delta\theta = 1.4^\circ$ , full width at half maximum.<sup>6</sup> These data then imply:

$$\sigma_2(\varphi) d\varphi = (1 - |\varphi|/\Delta\theta) (d\varphi/\Delta\theta), \quad (7)$$

for  $|\varphi| < \Delta\theta$ , and  $\sigma_2 = 0$  for  $|\varphi| > \Delta\theta$ .

In order to obtain a realistic form for  $\sigma_3(z)$ , the axial phase space distribution of the particles should be considered. Data on this distribution obtained from both internal and external beam measurements are available for the MSU cyclotron.<sup>6</sup> These data suggest a form for  $\sigma_3(z)$  having a symmetric trapezoidal shape with a full width of 0.75 cm and with  $\Delta z = 0.5$  cm, full width at half maximum. The results obtained for  $E_{sc}$  are insensitive to the detailed shape of  $\sigma_3$  and depend mainly on the value of  $\Delta z$ .

Because of the separated turn structure of the beam, the microscopic charge density is a rapidly oscillating function of radius. In the MSU cyclotron, the radial width of a single ion pulse is  $\delta R \cong 0.8$  mm while the radius gain per turn is  $\Delta R = 2.5$  mm at  $R = 50$  cm. Calculations of the longitudinal space charge effect which include this turn structure have also been carried out, and the results indicate that this micro-structure is not significant when:  $\delta R \ll \Delta z$ , and  $\Delta R \ll R\Delta\theta$ . These calculations are complicated and will not be discussed here.

## 5. ELECTRIC FIELD CALCULATIONS

In calculating the electric field we assume a two dimensional cartesian model in which  $y = R\varphi$  and  $\rho = \rho(y, z)$  at a given  $R$  value. Here,  $F_\theta(R, \varphi, z)$  is replaced by  $F_y(y, z)$  and  $R$  becomes simply a parameter. Eqn (6) is replaced by:

$$\rho(y, z) = F_0(\Delta y) K(R) \sigma_2(y) \sigma_3(z), \quad (8)$$

with  $\Delta y = R\Delta\theta$ , and  $\int \sigma_2(y) dy = 1$ . This model greatly simplifies the field calculation and can be justified when  $\Delta\theta$  is small. The analysis includes the effect of image charges by assuming that conducting planes at  $z = \pm z_d$  enclose the beam. In the MSU cyclotron, the two dees and one dummy dee, which have an aperture of 3.81 cm, enclose the beam for  $320^\circ$  of azimuth; it therefore seems reasonable to neglect the remaining  $40^\circ$  and to simply take  $2z_d = 3.81$  cm. These conducting planes are quite important since they cause the field contribution

310

from distant charge elements to fall off exponentially with distance, which then improves the validity of the model.

Assuming  $\rho(y, z)$  is an even function of  $z$ , then the electrostatic potential is given by the real part of the following function:

$$W(y, z) = -2 \int dy' dz' \rho(y', z') \ln[\tan k'(\xi - \xi')], \quad (9)$$

where  $k' = \pi/4z_d$ ,  $\xi = z + iy$ ,  $\xi' = z' + iy'$ . Taking the real part of  $(-\partial W/\partial y)$  yields:

$$F_y(y, z) = 2 \int dy' dz' \rho(y', z') (L_1/L_2), \quad (10)$$

where  $L_1 = k \cos \xi \sinh \eta$ ,  $L_2 = \sin^2 \xi + \sinh^2 \eta$ ,  $\xi = k(z' - z)$ ,  $\eta = k(y - y')$ , and  $k = \pi/2z_d$ .

The above expression can be cast into a form more suitable for computation by using Eqn (8) and introducing  $f(y - y', z)$  given by:

$$f(y - y', z) = (\Delta y) \int \sigma_3(z') (L_1/L_2) dz', \quad (11)$$

with  $L_1$  and  $L_2$  given above. This function, which is proportional to the field produced by an infinite charge strip of thickness  $dy'$  located at  $y'$ , is an odd function of  $(y - y')$  and has a discontinuity at  $y = y'$  for  $z \cong 0$ . To remove any difficulty arising from this discontinuity, the function  $G(y, z)$  is calculated from:

$$G(y, z) = \int [\sigma_2(y') - \sigma_2(2y - y')] f(y - y', z) dy', \quad (12)$$

where the integration extends from  $y' = -\infty$  only up to  $y' = y$ . A comparison with Eqn (10) then yields:

$$F_y(y, z) = 2F_0 K(R) G(y, z), \quad (13)$$

so that  $G$  is a dimensionless field function which is specified by the geometric parameters:  $R\Delta\theta$ ,  $\Delta z$ ,  $z_d$ .

Fig. 2 shows curves for  $G$  vs  $\varphi$  for  $R = 25$  and  $71$  cm ( $\tau = 25, 200$ ). These curves were obtained for the triangular  $\sigma_2$  and the trapezoidal  $\sigma_3$  discussed in Section 4. These curves show that  $G(\varphi)$  varies slowly with  $R$ ; indeed, the curve for  $R = 50$  cm ( $\tau = 100$ ) is almost indistinguishable from that shown for  $R = 71$  cm ( $\tau = 200$ ). The function  $G(\varphi)$  always approaches an asymptotic limit for  $R|\varphi| > z_d/2$ ; this is an important consequence of the image forces, which holds independent of the detailed shape of  $\sigma_2$  or  $\sigma_3$ . Making use of this conclusion and the definition of  $G$  in Eqn (13), we can then rewrite Eqn (3) as:

$$E_{sc}(\varphi) = 4\pi q F_0 G(R_0\varphi) \int R K(R) d\tau, \quad (14)$$

with  $R_0 \cong 0.7 R_{\max}$ . Thus, the  $\varphi$  dependence of  $E_{sc}$  is nearly identical to that of  $G$  evaluated at  $R_0$ .

For a given axial beam width  $\Delta z$ , the values of  $G(\varphi)$  decrease substantially as  $\Delta z \rightarrow 2z_d$ , the aperture of the surrounding conductors. This is shown in Fig. 3 which presents curves of  $G$  vs  $\varphi$  obtained for:  $2z_d = \infty, 3.81, 1.27$  cm, and with

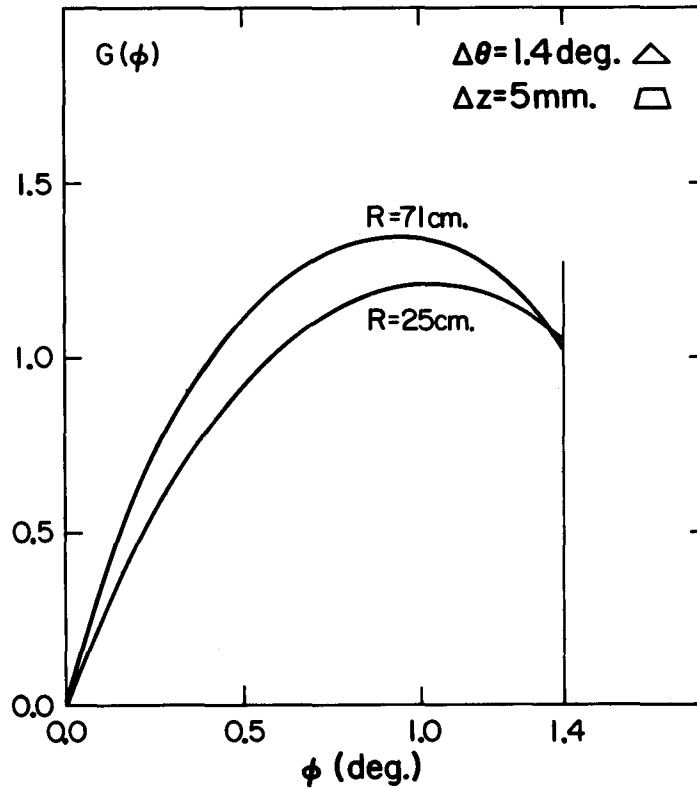


Fig. 2. Plots of field function  $G$  vs phase  $\phi$  at  $z = 0$ , obtained for  $R = 25$  cm and  $71$  cm. Charge distribution has triangular shape in azimuthal direction and trapezoidal shape in axial direction. Figure demonstrates slow variation of  $G(\phi)$  with  $R$  between turns 25 and 200

$\Delta z = 1$  cm. Moreover, the value of  $G$  falls off more sharply with increasing  $|z|$  when  $\Delta z \rightarrow 2z_d$ . These conclusions, which result from the effect of the image charges, hold quite generally and clearly indicate how the longitudinal space charge effect can be rendered harmless. When  $\Delta z \ll 2z_d$ , as is the case for the MSU cyclotron, then only  $G(\phi)$  values for  $z = 0$  need be considered. Excessively small values for  $\Delta z$  should certainly be avoided since  $G$  diverges logarithmically as  $\Delta z \rightarrow 0$ .

Fig. 4 presents  $G$  vs  $\phi$  curves for three different distributions: rectangular, trapezoidal, and triangular, all having  $\Delta\theta = 4^\circ$  (FWHM). These curves clearly demonstrate that the  $\phi$  dependence of  $G$ , and hence also that of  $E_{sc}$ , is quite non-linear and strongly dependent on the form of  $\sigma_2(\phi)$ .

### 5.1. Special formulas

For the rectangular distribution:  $\sigma_3(|z| < z_0) = \frac{1}{2} z_0$  and  $\sigma_3(|z| > z_0) = 0$ , the function  $f$  of Eqn (11) becomes simply:

$$f_0(y - y', z) = (\Delta y / 2z_0) [\tan^{-1} X_1 + \tan^{-1} X_2], \quad (15)$$

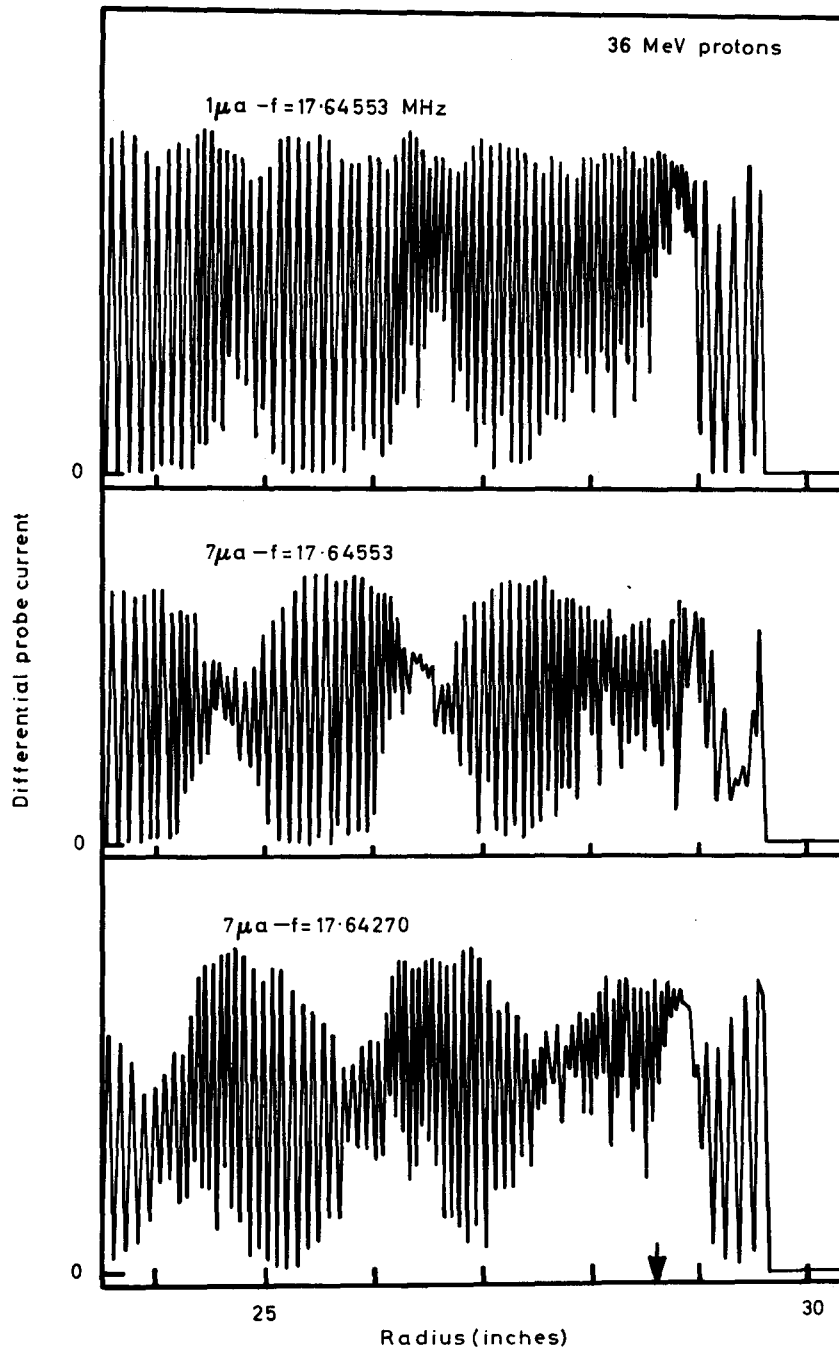


Fig. 5. Three differential probe 'turn patterns'. Top and middle pattern demonstrate that the longitudinal space charge effect destroys turn separation when the beam current increases from 1 to 7.2  $\mu\text{A}$ , while bottom pattern shows that turn separation can be restored by an appropriate frequency shift:  $\Delta f = -2.8 \text{ kHz}$ . Arrow at  $r = 28.61$  in shows location of the  $\nu_r = 1$  resonance

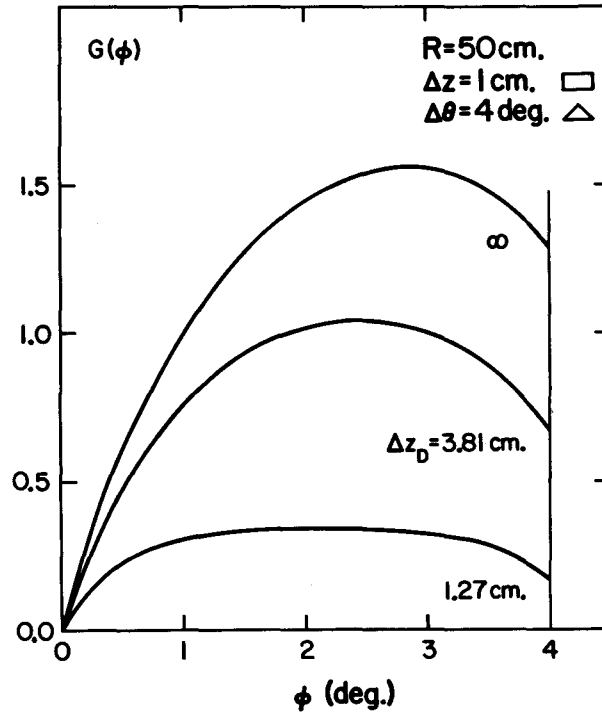


Fig. 3. Plots of field function  $G$  vs phase  $\phi$  at  $z = 0$  and  $R = 50$  cm. Charge distribution has triangular shape in azimuthal direction and rectangular shape in axial direction. Curves demonstrate dependence of  $G$  on conductor aperture:  $\Delta z_d = \infty, 3.81, 1.27$  cm when beam height is  $\Delta z = 1$  cm

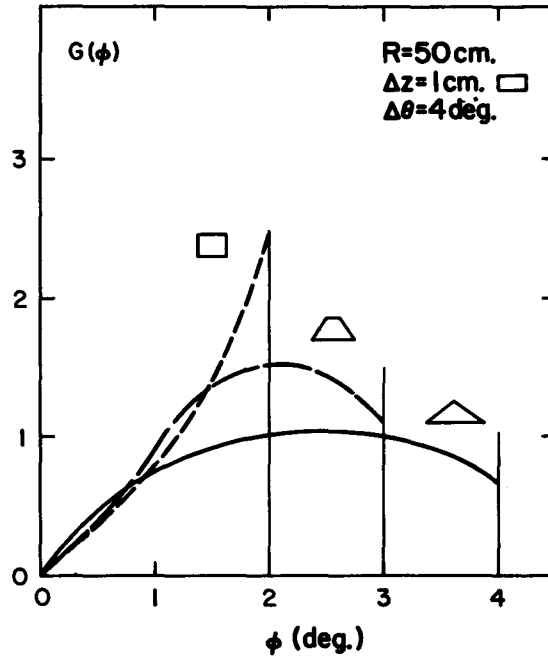


Fig. 4. Plots of field function  $G$  vs  $\phi$  at  $z = 0$  and  $R = 50$  cm. Charge distribution has rectangular shape in axial direction and different curves shown correspond to following shapes in azimuthal direction: rectangular, trapezoidal and triangular

where  $X_{1/2} = [\sin k(z_0 \pm z)] / \sinh \eta$ , and  $|\tan^{-1} X_{1/2}| < \pi/2$ . In this case, the evaluation of  $G(y, z)$  via Eqn (12) requires only one integration. If in addition,  $\sigma_2(y)$  is also a rectangular distribution with  $\Delta y = 2y_0 = 2R\Delta\theta$ , then the following approximate formula for  $G(y, z = 0)$  is obtained:

$$G_o(y) = U_2 \tan^{-1}(1/U_2) - U_1 \tan^{-1}(1/U_1) + (\frac{1}{2}) \ln[(1 + U_2^2)/(1 + U_1^2)] - \ln(T_1/T_2), \quad (16)$$

where:  $U_{2/1} = (y_0 \pm y)/z_0$ , and  $T_{2/1} = [\tanh k'(y_0 \pm y)] / (y_0 \pm y)$ , with  $k' = \pi/4z_d$ . The terms involving  $U_{2/1}$  represent an exact evaluation of the contribution from the charges between the conducting planes, while the last term is the contribution from all the image charges calculated only to zero order in  $z_0$ ; hence, this expression is valid only if  $z_0 \ll z_d$ . This  $G_o(y)$  can be used to quickly obtain estimates of the longitudinal space charge effect. It should also be noted that  $G$  can be explicitly evaluated (by solving Poisson's equation) for  $\sigma_3 \sim \cos(nkz)$  where  $n$  is any odd integer, with  $\sigma_2(y)$  having any simple analytical form.

## 6. DISCUSSION OF RESULTS

The experimental data and associated calculations presented here pertain specifically to the 36 MeV proton configuration of the cyclotron in which the peak energy gain per turn is 170 kV. The phase distribution within the beam is given by Eqn (7) with  $\Delta\theta = 1.4^\circ$ ; this implies a full energy width of 11 kV, and a width of 2.8 kV for 75% of the protons. Fig. 5 displays three 'turn patterns' obtained with the differential probe which cover about the last 50 turns inside the machine. The top pattern is for  $I = 1 \mu\text{A}$  with rf frequency  $f = 17.65 \text{ MHz}$  adjusted to yield minimum turn width at extraction. The middle pattern was obtained under identical conditions but with ion source output increased so that  $I = 7.2 \mu\text{A}$ ; the loss of turn separation here clearly demonstrates the longitudinal space charge effect. The bottom pattern was obtained under the same conditions as the middle one but with a frequency shift  $\Delta f = -2.8 \text{ kHz}$ , so chosen as to obtain again the sharpest turn definition; this result indicates that the space charge effect can be compensated by an appropriate frequency shift as discussed in Section 3. These figures are copies of the output from a strip chart recorder with a moving pen of limited resolution so that details of turn structure are lost. When these patterns were observed, the dee voltage regulation was  $\Delta V/V \cong 6 \times 10^{-4}$ , corresponding to an energy variation  $\Delta E \cong 22 \text{ kV}$ . Note that beyond  $\nu_r = 1$  some turns are missing from these patterns because of the precessional motion of the orbits which are driven off-centre at this resonance. Also, the differential probe is located  $160^\circ$  upstream from the deflector entrance.

More recently, the dee voltage regulation has been improved to:  $\Delta V/V = 2 \times 10^{-4}$ , corresponding to an energy variation of about 7 kV. With the slits of the beam transport-analysing system set to pass an energy slice of only  $\Delta E = 6 \text{ kV}$ , it was observed that for an internal beam of  $0.75 \mu\text{A}$ , a current of  $0.15 \mu\text{A}$  was transmitted, and when the internal beam was increased to  $6 \mu\text{A}$ , the transmitted current became  $0.6 \mu\text{A}$ . In each case the rf frequency was adjusted to yield the maximum transmission. Since the percentage transmission decreased from 20% to 10% when the internal beam current was increased, it must be concluded that the rf frequency adjustment only partly cancels the energy spread produced by the space charge effect.

Values of  $E_{sc}$  vs  $\phi$  were calculated using Eqns (3, 5, 13) with  $G(R\phi)$  functions displayed in Fig. 2. Because of the phase selection slits, the first 28 turns constitute the 'injector' for the remainder of the cyclotron; hence, the calculation of  $E_{sc}$  justifiably omitted these first 28 turns. In addition, the calculation approximated the contribution from the last 20 turns where the beam is in the non-isochronous extraction region and where  $F_\theta$  falls off to zero. A correction factor was also included which takes account of the increased number of turns produced by an rf frequency shift. The values of  $E_{rf}$  vs  $\phi$  were calculated from Eqn (4) with  $E_0 = 36$  MeV. The resultant value of  $E - E_0 = E_{sc} + E_{rf} - E_0$  then represents the energy displacement of particles with given  $\phi$  from those at the central phase evaluated at extraction.

The three  $(E - E_0)$  vs  $\phi$  curves presented in Fig. 6 were obtained for  $I = 1 \mu\text{A}$  and for frequency shifts:  $-\Delta f = 0.3, 0.9,$  and  $1.5$  kHz. In these three cases, the total energy spread is: 38, 26, and 50 kV respectively; while the percentage of particles with  $\Delta E < 6$  kV is: 5, 28, and 69% respectively. These results show why the rf frequency shift cannot fully compensate for the energy spread produced by the space charge effect.

The  $(E - E_0)$  vs  $\phi$  curves displayed in Fig. 7 represent an attempt to account for the observations reproduced in Fig. 5 and discussed above. It was assumed that the energy spread for  $I = 1 \mu\text{A}$  could be neglected so that the curves shown for

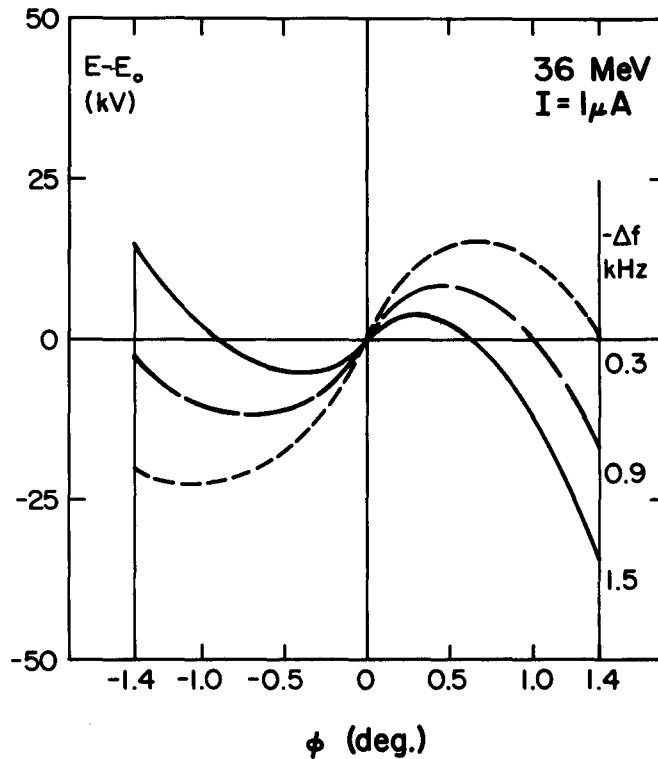


Fig. 6. Plots of energy displacement  $(E - E_0)$  vs phase  $\phi$  at  $E_0 = 36$  MeV as calculated from theory for  $I = 1 \mu\text{A}$  beam current. Different curves correspond to frequency shifts:  $-\Delta f = 0.3, 0.9,$  and  $1.5$  kHz. Figure demonstrates that frequency shift only partly cancels space charge effects

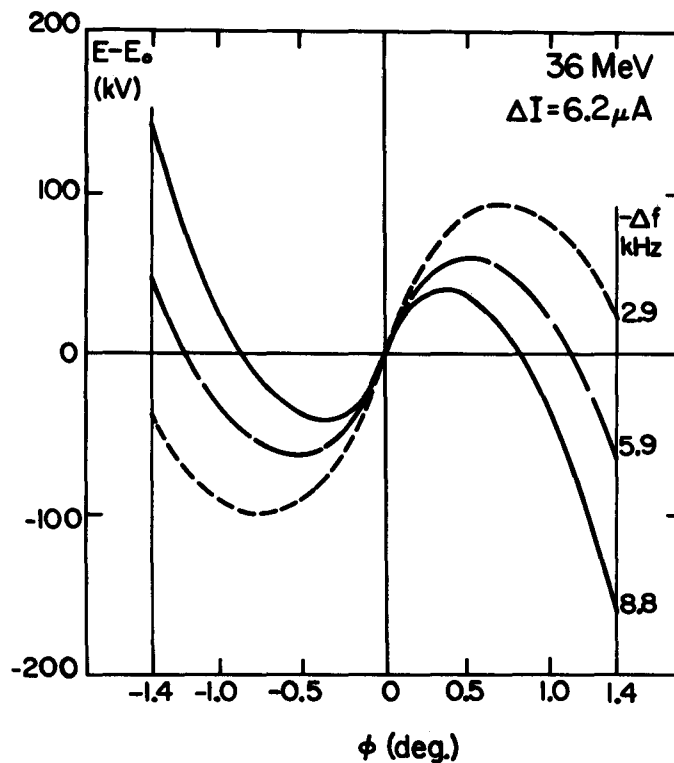


Fig. 7. Plots of  $(E - E_0)$  vs phase  $\phi$  at  $E_0 = 36$  MeV as calculated from theory for  $\Delta I = 6.2 \mu\text{A}$  increase in beam current. Different curves correspond to frequency shifts:  $-\Delta f = 2.9, 5.9,$  and  $8.8$  kHz. Compare with Figs 5 and 6

$\Delta I = 6.2 \mu\text{A}$  should actually correspond to the  $I = 7.2 \mu\text{A}$  data. Although the observed frequency shift was  $\Delta f = -2.8$  kHz, additional curves are shown for twice and thrice this value. These curves yield a full energy spread of  $\Delta E = 193, 128,$  and  $310$  kV respectively, with 50% of the particles having  $\Delta E < 152, 96,$  and  $62$  kV in the three cases. Since the observed frequency shift has only a small uncertainty, it must be concluded that the calculated  $E_{sc}$  values are about twice as large as required to fit this observation. This discrepancy may be accounted for by a partial neutralisation of the space charge produced by negative ions in the residual gas; at  $I = 7.2 \mu\text{A}$ , the beam density is  $2 \times 10^7$  protons/cm<sup>3</sup> which corresponds to a pressure of only  $10^{-5}$  torr, while the vacuum attained in the beam space is about  $10^{-5}$  torr; thus, if about one negative ion per  $10^4$  neutrals is present, these negative ions would significantly reduce the longitudinal space charge effect. Experimental and theoretical work on this problem will continue.

I am indebted to my colleague H. G. Blosser for supplying the experimental data and for his helpful discussions and suggestions. I am also grateful to D. A. Johnson for carrying out the computer work and preparing the figures.

DISCUSSION

Speaker addressed: M. M. Gordon (MSU)

*Question by V. P. Dmitrievsky (JINR Dubna):* What is the density of the space charge in the beam bunch?

*Answer:* The proton density is about  $10^7$  per c.c., that is a pressure of about  $10^{-9}$  torr. The tank pressure is not well known but is about  $10^{-5}$  torr, so that 1 negative ion per  $10^4$  neutrals will affect things.

*Question by K. V. Ettinger (Birmingham):* At what beam level does the compensated space charge effect begin?

*Answer:* This is not exactly determined, but probably at a level of about  $1 \mu\text{A}$ .

*Question by H. L. Hagedoorn (Technological University of Eindhoven):* Is the compensation of space charge effects such that we can speak about a 'homogeneous' space charge compensation by the produced negative ions?

*Answer:* I think this would be the most reasonable assumption.

*Question by M. Reiser (Maryland):* Do you include the effect of the bursts on all the other turns?

*Answer:* Yes, the details are given in the printed paper.

*Question by A. A. Kolomensky (Lebedev Institute):* Have you taken into account the influence of image forces?

*Answer:* Image forces have been taken into account in a rather elegant way, I believe!

REFERENCES

1. Gordon, M. M., *Nucl. Instr. Meth.* **58**, 245, (1968).
2. Rickey, Sampson, and Bardin, *I.E.E.E. Trans. Nucl. Sci.* (1969); to be published.
3. Welton, T. A., Sector-focused Cyclotrons, Nucl. Sci. Ser. Report No. 26, NAS-NRC-656, 192, (Washington, D.C., 1959).
4. Welton, T. A., private communication, (1958).
5. Powell, W. B., private communication, (September 1967).
6. Blosser, H. G., Proceedings of this Conference, p. 257.
7. Gordon, M. M., *I.E.E.E. Trans. Nucl. Sci.* NS-13, 48, (1966).
8. Courant, E. D., *Ann. Rev. Nucl. Sci.* **18**, 435, (1968).
9. Berg, Blosser, and Gordon, *Nucl. Instr. Meth.* **58**, 327, (1968).